Measurement of the CKM angle γ from $B^{\mp} \to D^{(*)}[K_s^0\pi^-\pi^+]K^{(*)\mp}$ decays in *BABAR*

F. Martínez-Vidal*
IFIC, Universitat de València-CSIC, E-46071 Valencia, Spain
(On behalf of the BaBar Collaboration)

We report on the measurement of the Cabibbo-Kobayashi-Maskawa angle γ through a Dalitz analysis of neutral D decays to $K_S^0\pi^-\pi^+$ in the processes $B^{\mp} \to D^{(*)}K^{\mp}$ and $B^{\mp} \to DK^{*\mp}$, $D^* \to D\pi^0, D\gamma$, with the *BABAR* experiment at SLAC asymmetric B-Factory.

I. INTRODUCTION AND OVERVIEW

The angle γ of the unitarity triangle is the phase of the Cabibbo-Kobayashi-Maskawa (CKM) matrix [1] defined as $\gamma \equiv \arg\left[-V_{ud}V_{ub}^*/V_{cd}V_{cb}^*\right]$, which corresponds to the phase of the element V_{ub}^*, i.e. $V_{ub} = |V_{ub}|e^{-i\gamma}$, in the Wolfenstein parameterization [2]. The precise measurement of the angle γ is a crucial goal of the physics program at B-factories, however, it is also one of the most difficult to achieve.

Among all methods proposed to extract γ, only those using $B^{\mp} \to \tilde{D}^0K^{\mp}$ decays are theoretically clean because the main contributions to the amplitudes come from tree-level diagrams, neglecting $D^0 - \overline{D}^0$ mixing [3] (the symbol $\tilde{D}^0$ indicates either a D^0 or a $\bar{D}^0$ meson). The interference between the color allowed $B^- \to D^0K^-$ ($b \to c\bar{u}s$) and the color suppressed $B^- \to \bar{D}^0K^-$ ($b \to u\bar{c}s$) transitions [4], when the D^0 and $\bar{D}^0$ are reconstructed in a common final state [5–8], introduces a relative phase γ in the decay amplitude. The sensitivity to γ depends on the magnitude of the ratio of the $b \to u\bar{c}s$ amplitude with respect to the $b \to c\bar{u}s$ one, r_B, which plays a key role on the ability to measure γ at B-factories. Theoretical expectations, consistent with current experimental limits, give $r_B \sim 0.1$.

When the $\tilde{D}^0$ is reconstructed in a 3-body final state with rich resonant structure, like $K_S^0\pi^-\pi^+$, the interference between doubly-Cabibbo suppressed, Cabibbo allowed and *CP*-eigenstate amplitudes provide strong phases to ensure the sensitivity to γ [7, 8]. The angle γ can then be extracted through an analysis of the distribution of the events in the $\tilde{D}^0$ Dalitz plane

Assuming negligible effects from $D^0 - \overline{D}^0$ mixing [3] and *CP* asymmetries in D decays [9], the $B^{\mp} \to \tilde{D}^{(*)0}K^{\mp}$, $\tilde{D}^0K^{*\mp}$, with $\tilde{D}^{*0} \to \tilde{D}^0\pi^0, \tilde{D}^0\gamma$, $\tilde{D}^0 \to K_S^0\pi^-\pi^+$ decay chain rate $\Gamma^{(*)}_{\mp,s\mp}(m_-^2, m_+^2)$ can be written using the following general parameterization [10],

$$\Gamma^{(*)}_{\mp,s\mp}(m_-^2, m_+^2) \propto |\mathcal{A}_{D\mp}|^2 + r_{B,s}^{(*)^2}|\mathcal{A}_{D\pm}|^2 + 2\epsilon\left\{x^{(*)}_{\mp,s\mp}\,\mathrm{Re}[\mathcal{A}_{D\mp}\mathcal{A}^*_{D\pm}] + y^{(*)}_{\mp,s\mp}\,\mathrm{Im}[\mathcal{A}_{D\mp}\mathcal{A}^*_{D\pm}]\right\}, \quad (1)$$

where m_-^2 and m_+^2 are the squared invariant masses of the $K_S^0\pi^-$ and $K_S^0\pi^+$ combinations, respectively, $\mathcal{A}_{D\mp} \equiv \mathcal{A}_D(m_\mp^2, m_\pm^2)$, with $\mathcal{A}_{D-}$ ($\mathcal{A}_{D+}$) the amplitude of the $D^0 \to K_S^0\pi^-\pi^+$ ($\overline{D}^0 \to K_S^0\pi^+\pi^-$) decay. We introduce the generalized *CP (cartesian) parameters* $x^{(*)}_{\mp,s\mp} = \kappa r^{(*)}_{B,s}\cos(\delta^{(*)}_{B,s} \mp \gamma)$ and $y^{(*)}_{\mp,s\mp} = \kappa r^{(*)}_{B,s}\sin(\delta^{(*)}_{B,s} \mp \gamma)$, verifying $x^{(*)^2}_{\mp,s\mp} + y^{(*)^2}_{\mp,s\mp} = \kappa^2 r^{(*)^2}_{B,s}$. The parameter κ accounts for interference between resonant and non-resonant K^* decays, as a consequence of the natural width of the K^*, with $0 \leq \kappa \leq 1$ [10]. For $B^{\mp} \to \tilde{D}^{(*)0}K^{\mp}$ decays, $\kappa = 1$. Here, $r^{(*)}_{B,s}$ is the magnitude of the ratio of the amplitudes $\mathcal{A}(B^- \to \bar{D}^{(*)0}K^-,\ \overline{D}^0K^{*-})$ and $\mathcal{A}(B^- \to D^{(*)0}K^-,\ D^0K^{*-})$ and $\delta^{(*)}_{B,s}$ is their relative strong phase. As a consequence of parity and angular momentum conservation in the $\tilde{D}^{(*)0}$ decay, the factor ϵ in Eq. (1) takes the value $+1$ for $B^{\mp} \to \tilde{D}^0K^{\mp}$, $\tilde{D}^{*0}[\tilde{D}^0\pi^0]K^{\mp}$, $\tilde{D}^0K^{*\mp}$, and -1 for $B^{\mp} \to \tilde{D}^{*0}[\tilde{D}^0\gamma]K^{\mp}$ [11]. The parameterization given by Eq. (1) is also valid in the case when r_s and δ_s happen to vary within the K^* mass window, and accounts for efficiency variations as a function of the kinematics of the B decay.

II. DATA SAMPLE AND EVENT SELECTION

The analysis for $B^- \to \tilde{D}^{(*)0}K^-$ ($B^- \to \tilde{D}^0K^{*-}$) decays [4] is based on a sample of approximately 347 (227) million $B\bar{B}$ pairs collected by the *BABAR* detector [12] at the SLAC PEP-II e^+e^- asymmetric-energy storage ring. For each B decay channel we also reconstruct its own control sample, $B^- \to \tilde{D}^{(*)0}\pi^-$ ($B^- \to \tilde{D}^0a_1^-$).

The reconstruction and selection criteria is described in detail elsewhere [13–15]. B meson candidates are characterized by using the energy difference ΔE, the beam-energy substituted mass m_{ES}, and a Fisher discriminant $\mathcal{F}$ to separate $e^+e^- \to q\bar{q}$, $q = u, d, s, c$ (continuum) and $B\overline{B}$ events [13]. If both $B^- \to \tilde{D}^{*0}[\tilde{D}^0\pi^0]K^-$ and $B^- \to \tilde{D}^{*0}[\tilde{D}^0\gamma]K^-$ candidates are selected in the same event, only the $B^- \to \tilde{D}^{*0}[\tilde{D}^0\pi^0]K^-$ is kept. The cross-feed among the different samples is negligible except for $B^- \to \tilde{D}^{*0}[\tilde{D}^0\gamma]K^-$, where the background from $B^- \to \tilde{D}^{*0}[\tilde{D}^0\pi^0]K^-$ is about 5% of the signal yield. This contamination has a negligible effect on the *CP* parameters.

The reconstruction efficiencies are 15%, 7%, 9%, and 11%, for the $B^- \to \tilde{D}^0K^-$, $B^- \to \tilde{D}^{*0}[\tilde{D}^0\pi^0]K^-$,

*Electronic address: `martinef@slac.stanford.edu`

$B^- \to \tilde{D}^{*0}[\tilde{D}^0\gamma]K^-$, and $B^- \to \tilde{D}^0 K^{*-}$ decay modes, respectively. Figure 1 shows the $m_{\rm ES}$ distributions after all selection criteria, for $|\Delta E| < 30(25)$ MeV, for $B^- \to \tilde{D}^{(*)0}K^-(B^- \to \tilde{D}^0 K^{*-})$. The largest background contribution is from continuum events or $B\overline{B}$ decays where a fake or true D^0 is combined with a random track. Another source of background for $B^- \to \tilde{D}^{(*)0}K^-$ is given by $B^- \to \tilde{D}^{(*)0}\pi^-$ decays where the prompt pion is misidentified as kaon. These decays are separated from the signal using their different ΔE distribution.

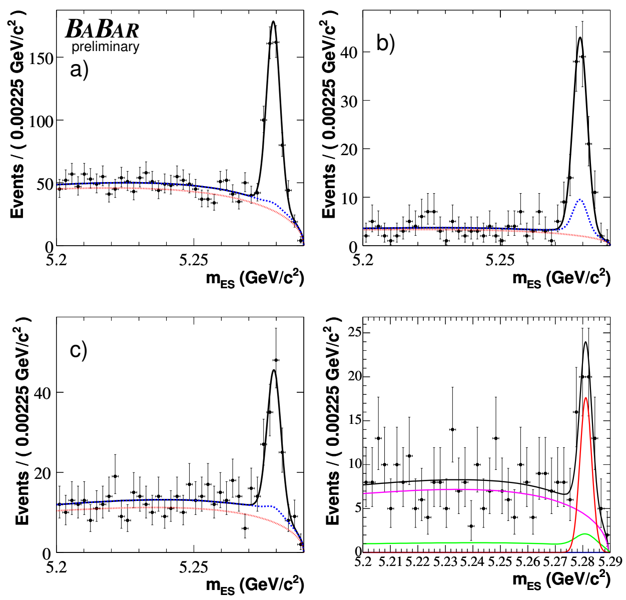

FIG. 1: Distributions of $m_{\rm ES}$ for (a) $B^- \to \tilde{D}^0 K^-$, (b) $B^- \to \tilde{D}^{*0}[\tilde{D}^0\pi^0]K^-$, (c) $B^- \to \tilde{D}^{*0}[\tilde{D}^0\gamma]K^-$, and (c) $B^- \to \tilde{D}^0 K^{*-}$. The curves superimposed represent the overall fit projections (solid black lines), the continuum contribution (dotted red lines), and the sum of all background components (dashed blue lines).

III. THE $D^0 \to K^0_S\pi^-\pi^+$ DECAY MODEL

The $D^0 \to K^0_S\pi^-\pi^+$ decay amplitude $\mathcal{A}_D(m^2_-, m^2_+)$ is determined from an unbinned maximum-likelihood fit to the Dalitz plot distribution of a high-purity (97.7%) tagged D^0 sample from 390328 $D^{*+} \to D^0\pi^+$ decays reconstructed in 270 fb^{-1} of data, shown in Fig. 2. Our phenomenological reference model to describe $\mathcal{A}_D(m^2_-, m^2_+)$ uses a sum of two-body amplitudes (subscript r) and a non-resonant (subscript NR) contribution,

$$\mathcal{A}_D(m^2_-, m^2_+) = \sum_r a_r e^{i\phi_r}\mathcal{A}_r(m^2_-, m^2_+) + a_{\rm NR}e^{i\phi_{\rm NR}}, \quad (2)$$

where the parameters a_r ($a_{\rm NR}$) and ϕ_r ($\phi_{\rm NR}$) are the magnitude and phase of the amplitude for component r (NR). The function $\mathcal{A}_r = F_r \times T_r \times W_r$ is the Lorentz-invariant expression that describes the dynamic properties of the D^0 meson decaying into $K^0_S\pi^-\pi^+$ through an intermediate resonance r, as a function of position in the Dalitz plane. Here, F_r is the Blatt-Weisskopf centrifugal barrier factor for the resonance decay vertex [16] with radius $R = 1.5$ GeV (0.3 fm), T_r is the resonant mass-lineshape, and W_r describes the angular distribution in the decay. For T_r we use a relativistic Breit-Wigner (BW) parameterization, except for $r = \rho(770)$ and $\rho(1450)$ where we use the functional form suggested in Ref. [17]. The angular dependence W_r is described with the helicity formalism as shown in [18][1]. Mass and width values are taken from [19], with the exception of $K^*_0(1430)^+$ taken from [20]. The model consists of a total of 13 resonances leading to 16 two-body decay amplitudes and phases (see Table I), and accounts for efficiency variations across the Dalitz plane and the small background contribution. All the resonances considered in this model are well established except the two scalar $\pi\pi$ resonances, σ and σ', whose masses and widths are obtained from our sample [21]. Their addition to the model is motivated by an improvement in the description of the data.

The possible absence of the σ and σ' resonances is considered in the evaluation of the systematic errors through the use of a K-matrix formalism [22] to parameterize the $\pi\pi$ S-wave states. The K-matrix method provides a direct way of imposing the unitarity constraint that is not guaranteed in the case of the BW model and is suited to the study of broad and overlapping resonances in multi-channel decays, avoiding the need to introduce the two σ scalars,

$$\mathcal{A}_D(m^2_-, m^2_+) = F_1(s) + \sum_{r \neq \pi\pi \;\; S=0} a_r e^{i\phi_r}\mathcal{A}_r(m^2_-, m^2_+), \quad (3)$$

where $F_1(s) = \sum_j \left[I - iK(s)\rho(s)\right]^{-1}_{1j} P_j(s)$ is the contribution of $\pi\pi$ S-wave states. Here, $s = m^2_{\pi^-\pi^+}$, I is the identity matrix, K is the matrix describing the S-wave scattering process, ρ is the phase-space matrix, and P is the initial production vector [22]. The index j represents the $j^{\rm th}$ channel ($1 = \pi\pi$, $2 = K\overline{K}$, $3 =$ multi-meson [23], $4 = \eta\eta$, $5 = \eta\eta'$). The K-matrix parameters are obtained from a global fit of the available $\pi\pi$ scattering data below 1900 MeV/c^2 [24], while the initial production vector is obtained from our fit to the tagged $D^0 \to K^0_S\pi^-\pi^+$ data.

IV. *CP* FIT RESULTS AND SYSTEMATIC UNCERTAINTIES

Once the decay amplitude $\mathcal{A}_D(m^2_-, m^2_+)$ is known it can be fed into Eq. (1). The extraction of the *CP*-violating parameters $x^{(*)}_{\mp,s\mp}$ and $y^{(*)}_{\mp,s\mp}$ is then performed

[1] The label A and B should be swapped in Eq. (6) of [18].

TABLE I: Complex amplitudes $a_r e^{i\phi_r}$ and fit fractions of the different components ($K_S\pi^-$, $K_S\pi^+$, and $\pi^+\pi^-$ resonances) obtained from the fit of the $D^0 \to K_S\pi^-\pi^+$ Dalitz distribution from $D^{*+} \to D^0\pi^+$ events. Errors are statistical only. The fit fraction is defined for the resonance terms as the integral of $a_r^2|\mathcal{A}_r(m_-^2, m_+^2)|^2$ over the Dalitz plane divided by the integral of $|\mathcal{A}_D(m_-^2, m_+^2)|^2$. The sum of fit fractions is 119.5%. A value different from 100% is a consequence of the interference among the amplitudes.

Component	$Re\{a_r e^{i\phi_r}\}$	$Im\{a_r e^{i\phi_r}\}$	Fraction (%)
$K^*(892)^-$	-1.223 ± 0.011	1.346 ± 0.010	58.1
$K_0^*(1430)^-$	-1.698 ± 0.022	-0.576 ± 0.024	6.7
$K_2^*(1430)^-$	-0.834 ± 0.021	0.931 ± 0.022	6.3
$K^*(1410)^-$	-0.25 ± 0.04	-0.11 ± 0.03	0.1
$K^*(1680)^-$	-1.285 ± 0.014	0.205 ± 0.013	0.6
$K^*(892)^+$	0.100 ± 0.004	-0.127 ± 0.003	0.5
$K_0^*(1430)^+$	-0.027 ± 0.016	-0.076 ± 0.017	0.0
$K_2^*(1430)^+$	0.019 ± 0.017	$0\ .177 \pm 0.018$	0.1
$\rho(770)$	1	0	21.6
$\omega(782)$	-0.0219 ± 0.0010	0.0394 ± 0.0007	0.7
$f_2(1270)$	-0.699 ± 0.018	0.387 ± 0.018	2.1
$\rho(1450)$	0.25 ± 0.04	0.04 ± 0.06	0.1
Non-resonant	-0.99 ± 0.19	3.82 ± 0.13	8.5
$f_0(980)$	0.447 ± 0.006	0.257 ± 0.008	6.4
$f_0(1370)$	0.95 ± 0.11	-1.619 ± 0.011	2.0
σ	1.28 ± 0.02	0.273 ± 0.024	7.6
σ'	0.290 ± 0.010	-0.066 ± 0.010	0.9

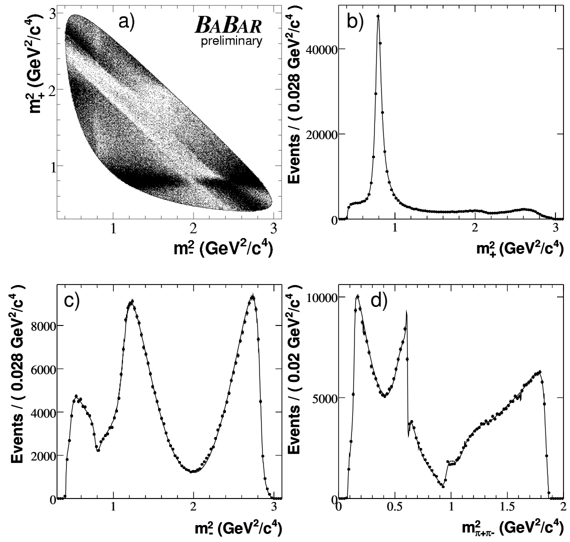

FIG. 2: (a) The $\bar{D}^0 \to K_S^0\pi^-\pi^+$ Dalitz distribution from $D^{*-} \to \bar{D}^0\pi^-$ events, and projections on (b) $m_+^2 = m_{K_S^0\pi^+}^2$, (c) $m_-^2 = m_{K_S^0\pi^-}^2$, and (d) $m_{\pi^+\pi^-}^2$. $D^0 \to K_S^0\pi^+\pi^-$ from $D^{*+} \to D^0\pi^+$ events are also included. The curves are the reference model fit projections.

through a simultaneous maximum likelihood fit to the $\Gamma_{-,s}^{(*)}(m_-^2, m_+^2)$ and $\Gamma_{+,s}^{(*)}(m_-^2, m_+^2)$ Dalitz plot distributions for $B^- \to \tilde{D}^{(*)0}K^-$ and $B^+ \to \tilde{D}^{(*)0}K^+$ decays, respectively. Experimentally, it was demonstrated that $x_{\mp,s\mp}^{(*)}$ and $y_{\mp,s\mp}^{(*)}$ are well behaving parameters, unbiased with Gaussian errors [13]. Different background components are considered: continuum, $B^- \to D^{(*)0}\pi^-$ for $B^- \to D^{(*)0}K^-$ only, and $B\overline{B}$. The likelihood function uses the Dalitz plot distribution (after correction for efficiency variations), $m_{\rm ES}$, ΔE, and $\mathcal{F}$, with shapes determined directly from the *CP* and control samples, from both signal and sideband regions. Only the shapes for $B\overline{B}$ background events are determined from Monte Carlo simulation. Events falling into the continuum and $B\overline{B}$ background components are themselves divided into events with a real or a fake (combinatorial) D^0. We finally account for the correlation between the flavor of true D^0 mesons and the charge of combinational charged kaon.

The signal yields measured with the *CP* fit are 398 ± 23, 97 ± 13, 93 ± 12, and 42 ± 8, for $B^- \to \tilde{D}^0K^-$, $B^- \to \tilde{D}^{*0}[\tilde{D}^0\pi^0]K^-$, $B^- \to \tilde{D}^{*0}[\tilde{D}^0\gamma]K^-$, and $B^- \to \tilde{D}^0K^{*-}$, respectively. The results for the *CP*-violating parameters $x_{\mp,s\mp}^{(*)}$ and $y_{\mp,s\mp}^{(*)}$ are summarized in Table II. The only non-zero statistical correlations involving the *CP* parameters are for the pairs (x_-, y_-), (x_+, y_+), (x_-^*, y_-^*), (x_+^*, y_+^*), (x_{s-}, y_{s-}), (x_{s+}, y_{s+}), which amount to -1%, 1%, -17%, -14%, -10%, and 2%, respectively. Figure 3 shows the one- and two-standard deviation confidence-level contours (including statistical and systematic uncertainties) in the (x, y) planes for all the reconstructed modes, and separately for B^- and B^+ decays. The separation (overlap) of the $(x_{-,s-}^{(*)}, y_{-,s-}^{(*)})$ and $(x_{+,s+}^{(*)}, y_{+,s+}^{(*)})$ confidence contours in these planes is an indication of direct *CP* violation (conservation).

The largest single contribution to the systematic uncertainties on the *CP* parameters comes from the choice of the Dalitz model used to describe the $D^0 \to K_S^0\pi^-\pi^+$ decay amplitude. We use a set of alternative models where some resonances are removed or the parameterization of the different waves are changed. For the $\pi\pi$ S-wave we use the K-matrix approach described in Sec. III, while for the P-wave we change the mass and width describing the $\rho(770)$ within their quoted uncertainty [19]. The uncertainty on the description of the $K\pi$ S-wave is estimated by floating in our flavor tagged D^0 sample the mass and width of the BW describing the $K^*(1430)$, and using an additional parameterization taken from Ref. [25] with parameters extracted from our fit. Since the $K\pi$ P-wave is dominated by the $K^*(892)$ in both Cabibbo allowed and doubly Cabibbo suppressed amplitude, the mass and the width of this resonance, taken from [19] in the reference model, are changed to the values obtained from our fit to the tagged D^0 sample. The resulting values are consistent with what is found in $B \to J/\Psi K\pi$ decays selected in *BABAR* data. For the $\pi\pi$ and $K\pi$ D-waves, described by the $f_2(1270)$ and $K_2^*(1430)$ resonances, respectively, we use as alternative the formalism derived from Zemach tensors [26]. The difference is very small for P-waves but is larger for D-waves. Other alternative models are built by removing the Blatt-Weisskopf penetration fac-

TABLE II: *CP*-violating parameters $x^{(*)}_{\mp,s\mp}$ and $y^{(*)}_{\mp,s\mp}$ obtained from the *CP* fit. The first error is statistical, the second is experimental systematic uncertainty and the third is the systematic uncertainty associated with the Dalitz model.

CP parameter	$B^- \to \tilde{D}^0 K^-$	$B^- \to \tilde{D}^{*0} K^-$	$B^- \to \tilde{D}^0 K^{*-}$
$x^{(*)}_{-,s-}$	$0.041 \pm 0.059 \pm 0.018 \pm 0.011$	$-0.106 \pm 0.091 \pm 0.020 \pm 0.009$	$-0.20 \pm 0.20 \pm 0.11 \pm 0.03$
$y^{(*)}_{-,s-}$	$0.056 \pm 0.071 \pm 0.007 \pm 0.023$	$-0.019 \pm 0.096 \pm 0.022 \pm 0.016$	$0.26 \pm 0.30 \pm 0.16 \pm 0.03$
$x^{(*)}_{+,s+}$	$-0.072 \pm 0.056 \pm 0.014 \pm 0.029$	$0.084 \pm 0.088 \pm 0.015 \pm 0.018$	$-0.07 \pm 0.23 \pm 0.13 \pm 0.03$
$y^{(*)}_{+,s+}$	$-0.033 \pm 0.066 \pm 0.007 \pm 0.018$	$0.096 \pm 0.111 \pm 0.032 \pm 0.017$	$-0.01 \pm 0.32 \pm 0.18 \pm 0.05$

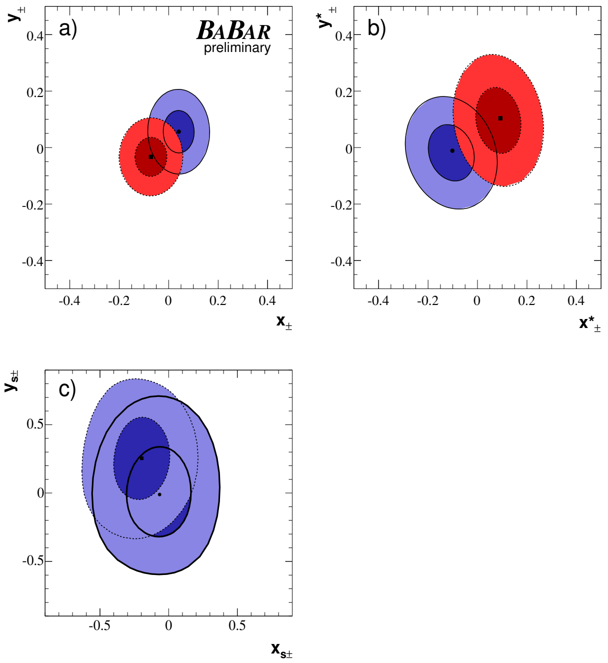

FIG. 3: Contours at 39.3% (dark) and 86.5% (light) confidence level (corresponding to two-dimensional one- and two-standard deviation regions), including statistical and systematic uncertainties, for (a) $(x_\mp, y_\mp)$, (b) $(x^*_\mp, y^*_\mp)$, and (c) $(x_{s\mp}, y_{s\mp})$ parameters, for B^- (thick and solid lines) and B^+ (thin and dotted lines) decays.

tors [16], removing resonances with small fit fractions $-K^*_2(1430)$, $K^*(1680)$, $K^*(1410)$ and $\rho(1450)$–, and replacing the running width of the BW by a fixed value. As (conservative) total systematic uncertainty associated with the Dalitz model, given in Table II, we consider the sum square of contributions from each alternative model, where each contribution is evaluated from the difference between the *CP* fit parameters using the alternative and the reference models. The dominant contributions to the overall Dalitz model uncertainty arise from the $\pi\pi$ andd $K\pi$ S-waves, and the fixed BW width.

Experimental systematic uncertainties arise from several sources, and can be found in Table III. All of them are small compared with the statistical precision, and their sum is similar to the Dalitz model uncertainty. Other possible sources of experimental systematic uncertainty are found to be negligible.

V. INTERPRETATION AND CONCLUSIONS

A frequentist (Neyman) procedure [13, 19, 27] has been adopted to interpret the measurement of the *CP* parameters $(x^{(*)}_\mp, y^{(*)}_\mp)$ reported in Table II in terms of confidence regions on $\mathbf{p} = (\gamma, r_B, \delta_B, r^*_B, \delta^*_B)$. No attempt has been done yet to include in the combination the *CP* parameters for $B^\mp \to DK^{*\mp}$ decays, $(x_{s\mp}, y_{s\mp})$. Figure 4 shows the two-dimensional projections onto the $r_B - \gamma$ and $r^*_B - \gamma$ planes of the one- and two-standard deviation regions, including statistical and systematic uncertainties. The figure reveals the two-fold ambiguity of this method, $(\gamma, \delta^{(*)}_{B,s}) \to (\gamma + 180°, \delta^{(*)}_{B,s} + 180°)$, as expected from Eq. (1). From the one-dimensional projections we obtain for the weak phase $\gamma = (92 \pm 41 \pm 11 \pm 12)°$, and for the strong phase differences $\delta_B = (118 \pm 63 \pm 19 \pm 36)°$ and $\delta^*_B = (-62 \pm 59 \pm 18 \pm 10)°$. No constraints on the phases are achieved at two standard deviation level and beyond. Similarly, for the magnitude of the ratio of decay amplitudes r_B and r^*_B we obtain the one (two) standard deviations constraints $r_B < 0.140$ ($r_B < 0.195$) and $0.017 < r^*_B < 0.203$ ($r^*_B < 0.279$). No constraint on γ is obtained from $B^\mp \to DK^{*\mp}$ decays alone, for which $\kappa r_s < 50(0.75)$ at one (two) standard deviation level. All these results are obtained considering the statistical correlations discussed in Sec. IV, while the experimental and Dalitz model systematic uncertainties are taken uncorrelated. We have verified that accounting for experimental systematic correlations within a given B decay channel, $(x_\mp, y_\mp)$, $(x^*_\mp, y^*_\mp)$, or $(x_{s\mp}, y_{s\mp})$, or assuming the experimental and Dalitz model systematic uncertainties between $(x_\mp, y_\mp)$ and $(x^*_\mp, y^*_\mp)$ fully correlated, has a negligible effect on the results.

In conclusion, *BABAR* has reached a good precision in the measurement of the *CP* parameters $(x^{(*)}_\mp, y^{(*)}_\mp)$ but the improvement of the error on γ (statistical and systematic) also depends on the value of the r_B parameter. Our last experimental results for $r^{(*)}_B$ are somewhat smaller than in our previously published analysis [13], Therefore, an improved precision in the determination of r_B is fundamental to better constraint γ. In this respect, the analysis of more data being recorded by the detector, the addition of more B (e.g. $B^\mp \to DK^{*\mp}$) and

TABLE III: Summary of the main contributions to the experimental systematic error on the CP parameters.

Source	x_-	y_-	x_+	y_+	x_-^*	y_-^*	x_+^*	y_+^*	x_{s-}	y_{s-}	x_{s+}	y_{s+}
$m_{\rm ES}$, ΔE, $\mathcal{F}$ shapes	0.002	0.004	0.003	0.004	0.011	0.012	0.008	0.008	0.08	0.12	0.10	0.12
Real D^0 fractions	0.002	0.000	0.000	0.000	0.002	0.003	0.002	0.016	0.03	0.03	0.03	0.04
Charge-D^0 flavor correlation	0.008	0.002	0.002	0.002	0.005	0.005	0.001	0.022	0.03	0.04	0.03	0.05
Efficiency in the Dalitz plot	0.014	0.000	0.013	0.001	0.001	0.002	0.000	0.001	0.06	0.04	0.07	0.09
Background Dalitz shape	0.006	0.003	0.001	0.004	0.012	0.015	0.009	0.009	0.04	0.09	0.04	0.09
Dalitz amplitudes and phases	0.004	0.004	0.004	0.004	0.008	0.008	0.008	0.008	0.01	0.01	0.01	0.01
$B^- \to D^{*0}K^-$ cross-feed	0.000	0.000	0.000	0.000	0.004	0.001	0.004	0.004	–	–	–	–
CP violation in $D\pi$ and $B\overline{B}$ bkg	0.000	0.000	0.000	0.000	0.005	0.002	0.002	0.005	0.00	0.00	0.00	0.00
Total experimental	0.018	0.007	0.014	0.007	0.020	0.022	0.015	0.032	0.11	0.16	0.13	0.18

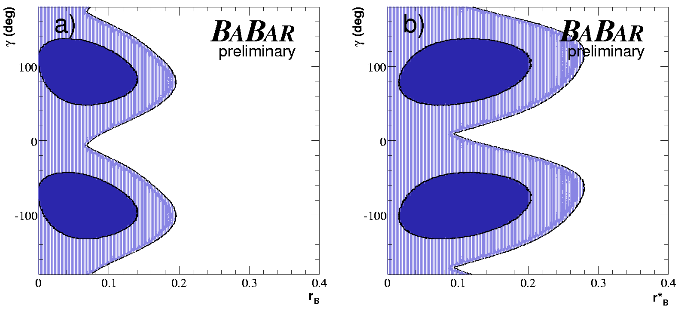

FIG. 4: Projections in the (a) $r_B - \gamma$ and (b) $r_B^* - \gamma$ planes of the five-dimensional one- (dark) and two- (light) standard deviation regions.

D (e.g. $D^0 \to \pi^0\pi^-\pi^+, K_S^0K^-K^+$) decay channels, and the combination with other methods [5, 6] will be helpful. Asuming $r_B \approx 0.1$ it will be possible to measure γ with 10° error with a 1 ab^{-1} data sample, which is within the reach of the *BABAR* experiment.

Acknowledgments

The author wish to thank the Spanish MEC under grant FPA2005-05142 for the support for this work.

[1] N. Cabibbo, Phys. Rev. Lett. **10**, 531 (1963); M. Kobayashi and T. Maskawa, Prog. Theor. Phys. **49**, 652 (1973).
[2] L. Wolfenstein, Phys. Rev. Lett. **51**, 1945 (1983).
[3] Y. Grossman, A. Soffer, J. Zupan, Phys. Rev. D 72, 031501 (2005).
[4] Reference to the charge-conjugate state is implied here and throughout the text unless otherwise specified.
[5] M. Gronau and D. London, Phys. Lett. B **253**, 483 (1991); M. Gronau and D. Wyler, Phys. Lett. B **265**, 172 (1991);
[6] D. Atwood, I. Dunietz and A. Soni, Phys. Rev. Lett. **78**, 3257 (1997).
[7] A. Giri, Y. Grossman, A. Soffer and J. Zupan, Phys. Rev. D **68**, 054018 (2003).
[8] Belle Collaboration, A. Poluetkov *et al.*, Phys. Rev. D **70**, 072003 (2004).
[9] CLEO Collaboration, D. M. Asner *et al.*, Phys. Rev. D **70**, 091101 (2004).
[10] M. Gronau, Phys. Lett. **B557**, 198 (2003).
[11] A. Bondar and T. Gershon, Phys. Rev. D **70**, 091503 (2004).
[12] *BABAR* Collaboration, B. Aubert *et al.*, Nucl. Instrum. Methods **A479**, 1-116 (2002).
[13] *BABAR* Collaboration, B. Aubert *et al.*, Phys. Rev. Lett. **95**, 121802 (2005).
[14] *BABAR* Collaboration, B. Aubert *et al.*, hep-ex/0507101.
[15] *BABAR* Collaboration, B. Aubert *et al.*, hep-ex/0607104.
[16] J. M. Blatt, V. F. Weisskopf, “Theoretical Nuclear Physics”, John Wiley & Sons, New York (1952).
[17] G.J. Gounaris and J.J. Sakurai, Phys. Rev. Lett. **21**, 244 (1968).
[18] CLEO Collaboration, S. Kopp *et al.*, Phys. Rev. D **63**, 092001 (2001).
[19] Particle Data Group, S. Eidelman *et al.*, Phys. Lett. B **592**, 1 (2004).
[20] E791 Collaboration, E. M. Aitala *et. al.*, Phys. Rev. Lett. **89**, 121801 (2002).
[21] The σ and σ' masses and widths are determined from the data. We find (in MeV/c^2) $M_\sigma = 490 \pm 6$, $\Gamma_\sigma = 406 \pm 11$, $M_{\sigma'} = 1024 \pm 4$, and $\Gamma_{\sigma'} = 89 \pm 7$. Errors are statistical.
[22] I. J. R. Aitchison, Nucl. Phys. A **189**, 417 (1972).
[23] Multi-meson channel refers to a final state with four pions.
[24] V.V. Anisovich and A.V. Sarantsev, Eur. Phys. Jour. **A16**, 229 (2003).
[25] LASS Collaboration, D. Aston *et al.*, Nucl. Phys. B **296**, 493 (1988).
[26] V. Filippini, A. Fontana and A. Rotondi, Phys. Rev. D **51**, 2247 (1995).
[27] J. Neyman, Phil. Trans. Royal Soc. London, Series A, **236**, 333 (1937), reprinted in *A selection of Early Statistical Papers on J. Neyman* (University of California Press, Berkeley, 1967).